

# Reversible Photoswitching of Donor–Acceptor Stenhouse Adducts in Water

Francisco G. Blandón-Cumbreras, Marek Jurtík, Aneta Závodná, Petr Janovský, Michal Rouchal\*, Robert Vícha, and Uwe Pischel\*



Cite This: <https://doi.org/10.1021/jacs.5c19813>



Read Online

ACCESS |

Metrics & More

Article Recommendations

Supporting Information

**ABSTRACT:** Adamantane-substituted donor–acceptor Stenhouse adducts (DASA) form highly stable host–guest complexes with cucurbit[*n*]urils (*n* = 7, 8) in water. These assemblies show kinetic stabilization of the colored linear form and, remarkably, exhibit reversible T-type photoswitching in water. These so far elusive features for first-generation DASA reveal a strategy for their potential use in biorelevant contexts.

Molecular photoswitches have been in the limelight of the design of stimuli-responsive (supra)molecular systems. This attraction builds on the spatiotemporal control exerted by light and the diversity of photoswitches. The most popular platforms are based on *E/Z* isomerization as found in azobenzenes and hemithioindigos or rely on ring-opening and -closing reactions, typical for spiropyrans, fulgimides or diarylethenes.<sup>1,2</sup> Donor–acceptor Stenhouse adducts (DASA), whose photochromic properties were first reported in 2014,<sup>3,4</sup> form part of the latter group. The stable linear form of these photoswitches is colored and is converted by visible-light irradiation into a colorless closed cyclopentenone form (see Scheme 1).<sup>5–7</sup> In organic solvents, such as toluene, the closed form may revert back to the linear form in a thermal process, known as T-type switching. The colored linear form tends to be more stable in organic media when presenting increased charge-transfer (CT) character, which is typical for first-generation DASA. However, this often penalizes the photo-induced multistep isomerization to the closed form.<sup>8</sup> To optimize the interplay of electronic/structural factors and molecular properties, various generations of DASA photoswitches were developed by tuning donor and acceptor moieties as well as the triene backbone.<sup>4,9–15</sup> This molecular diversity has sparked interest in the exploitation of the DASA platform in light-activatable materials,<sup>8,16–18</sup> photocontrolled phase-transfer,<sup>19</sup> drug delivery,<sup>20,21</sup> sensing<sup>22,23</sup> or photopharmacology.<sup>24</sup> However, such applications are foremost limited to organic environments (solvents, polymeric materials, *etc.*), while the use of DASA photoswitches in water has been much less successful.<sup>25,26</sup> The underlying reason is the spontaneous “dark switching” to the closed cyclopentenone form in polar protic media, occurring in the absence of light.<sup>5,27</sup> Beside other strategies,<sup>28</sup> it was reported that supramolecular encapsulation of a DASA chromophore could alleviate the undesired “dark switching” in water.<sup>24,29,30</sup> For example, a cyclodextrin host can stabilize the linear isomer of a second-generation DASA to some extent.<sup>24</sup> However, rather high concentrations of the photoswitch and host macrocycle as well as acidic pH were required and even then only *ca.* 1% of

the linear form was present. In a different approach it was shown that second-generation DASA, containing a tethered amine donor, can be reversibly switched in aqueous medium.<sup>28</sup> However, a significant amount of organic cosolvent is necessary, *i.e.*, 60 vol% tetrahydrofuran (THF). Hence, the switching of DASA in polar protic solvents remains a challenging task.<sup>8,26,28,31</sup>

The notion that steric hindrance by voluminous substituents at the amino donor site can disfavor the thermal steps that lead to the formation of the closed cyclopentenone form (Scheme 1) has been experimentally and theoretically cultivated in the literature.<sup>7,13,32</sup> However, this was not shown so far for DASA in water in the context of avoiding “dark switching”. Being conscious that the synthesis of DASA with sterically overcrowded amino donors is a nontrivial task,<sup>32</sup> we propose an alternative approach. We hypothesize that the site-selective encapsulation of the amino donor by a strongly binding macrocycle, such as a cucurbit[*n*]uril (CB*n*),<sup>33,34</sup> would exert the desired steric hindrance, while leaving the remaining chromophore in a nonconfined environment. It is noteworthy that cucurbit[*n*]urils have already found application in biorelevant contexts.<sup>33–35</sup>

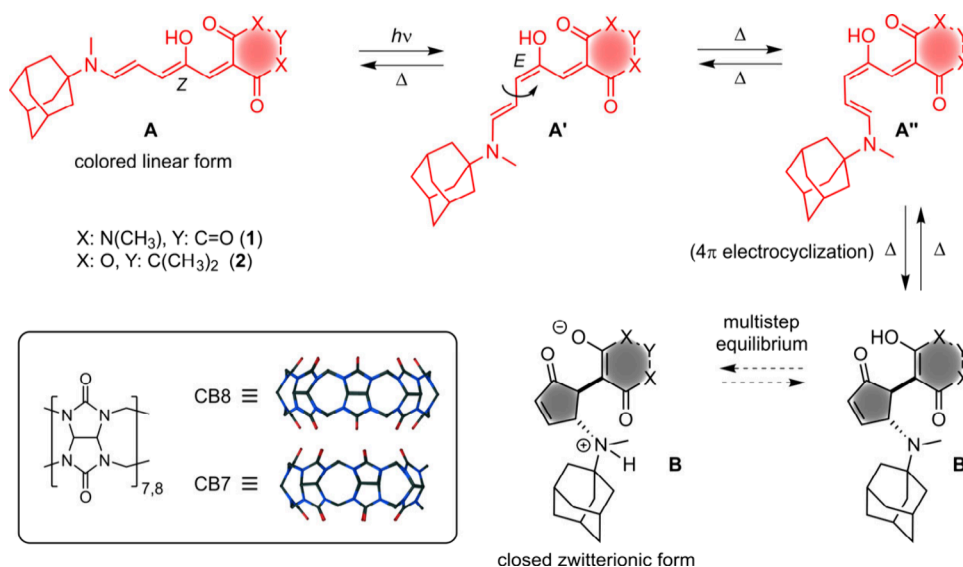
The pronounced CT character of first-generation DASA has been suggested to be the main obstacle for achieving reversible photoswitching in polar protic media.<sup>28</sup> Herein we demonstrate that significant steric effects can overrule the electronic effects, yielding the recyclable operation of DASA in water.

We designed the first-generation DASA derivatives **1** and **2** (Scheme 1), containing an adamantylamine donor and an acceptor derived from barbituric acid or Meldrum’s acid, respectively (see the Supporting Information for details about

**Received:** November 7, 2025

**Revised:** December 12, 2025

**Accepted:** December 16, 2025

Scheme 1. Structures of DASA Photoswitches 1 and 2 and General Switching Mechanism<sup>a</sup>

<sup>a</sup>The inset shows the structures of the employed CB<sub>n</sub> macrocycles. The mechanistic scheme is partially adapted from ref 26. Copyright 2025 American Chemical Society.

the synthesis and analytical characterization, Figures S1–S10). The choice of the adamantylamine was motivated by the generally accepted notion that 1-aminoadamantane forms highly stable host–guest complexes with CB<sub>n</sub> macrocycles ( $n = 7, 8$ ; CB7 and CB8 structures are shown in Scheme 1) at the level of nanomolar to femtomolar affinity ( $K$  ca.  $1.0 \times 10^{15} \text{ M}^{-1}$  for CB7 and  $8.2 \times 10^9 \text{ M}^{-1}$  for CB8) in water.<sup>36</sup> DFT calculations<sup>37,38</sup> established the adamantane moiety as preferred binding site of CB7 and CB8 for both isomers of 1 and 2; see Figure 1 for a graphical representation and the

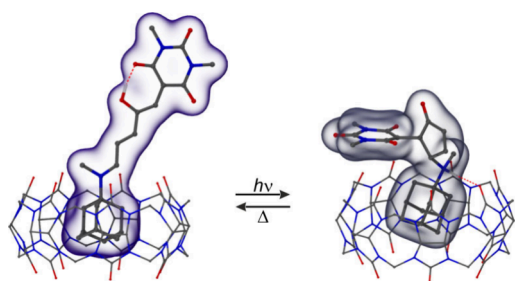


**Figure 1.** DFT-optimized structures of the CB7 complexes with 1 in the linear (left) and closed form (right).

Supporting Information (Table S2). The formation of host–guest complexes with CB7 and CB8 was further confirmed by mass spectrometry (Supporting Information, Figures S11–S14) and UV/vis absorption spectroscopy (see below).

To demonstrate the CT character of the linear form of 1 and 2, the UV/vis absorption spectra in solvents of varying polarity were recorded. It is well established that DASA photoswitches show negative solvatochromism and hence, in more polar solvents a blue-shift of the  $\pi, \pi^*$  absorption band is observed.<sup>8,26,39</sup> The longest-wavelength absorption maximum was plotted against the Dimroth-Reichardt parameter  $E_T^N(30)$  and the solvatochromic slope was determined, according to reported practice for DASA photoswitches.<sup>40</sup> For 1 and 2 a slope of  $-79 \text{ nm}$  and  $-65 \text{ nm}$ , respectively, resulted (Supporting Information, Figures S17–S18), which manifests

the significant CT nature of the linear form.<sup>40</sup> Interestingly, the addition of one equivalent CB7 to a solution of 1 or 2 in water produced a blue-shift by about 18–25 nm (Supporting Information, Table S1 and Figures S19 and S20). Likely, this effect is caused by the stabilization of the CT-related partial positive charge at the amine nitrogen atom by ion-dipole interactions with the carbonyl-lined CB7 portal. This observation provides additional hint on the successful complexation of the adamantylamine moiety by the macrocycle. For the larger CB8 macrocycle these effects were also evident, albeit being somewhat less pronounced (blue-shift by 8–9 nm).

To investigate the “dark switching”<sup>5,27</sup> of DASA 1 and 2, the colored linear form was dissolved in THF and then diluted into water, resulting in 10 vol% THF as cosolvent. The half-life ( $t_{1/2}$ ) of the linear form of DASA 1 is only about 38 min, as determined by monitoring the disappearance of the longest-wavelength absorption band (Figure 2). For DASA 2 a similarly short  $t_{1/2}$  of 29 min resulted (Supporting Information, Figure S25). Upon decolorization of the solution, new absorption features between 250 and 300 nm were observed, coincident with the reported spectral signature of the colorless cyclopentenone form.<sup>5</sup> However, when one equivalent of CB7 or CB8 was present (here no THF as cosolvent was needed), the “dark switching” was significantly altered. Initially ca. 25–30% of the dye was present in the linear form (assuming a molar absorption coefficient of  $\epsilon = 110\,000 \text{ M}^{-1} \text{ cm}^{-1}$ ) and the decolorization was considerably slowed down. For example, for DASA 1 a  $t_{1/2}$  of 12.4 h was determined for the host–guest complex with CB7, corresponding to a stability enhancement by a factor of about 20 (Figure 2). In the case of DASA 2 the effect was even more dramatic, leading to a  $t_{1/2}$  of 586.3 h and the observation that the supramolecular complex was about 1200 times more stable than the free dye (Supporting Information, Figure S29)! For the larger CB8 macrocycle also considerable benefits for the stabilization of the linear form of 1 and 2 applied, with  $t_{1/2}$  reaching values of 45.1 and 112.2 h, respectively (Supporting Information, Figures S28 and S30). The significantly slower “dark switching” in the presence

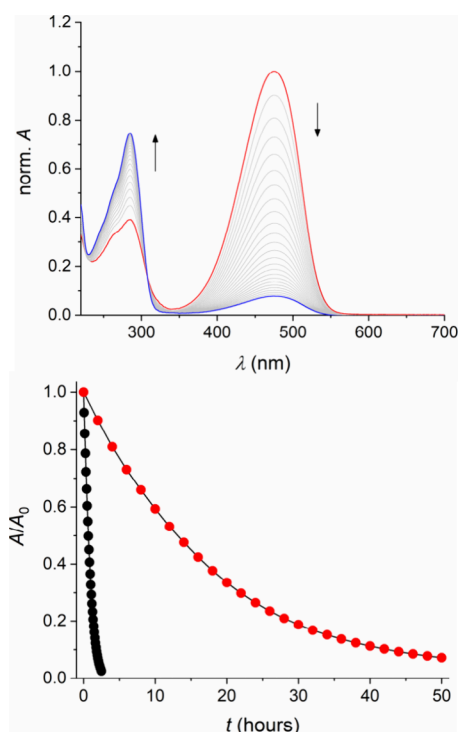


**Figure 2.** “Dark switching” of DASA 1 in water. Top: Spectral evolution in the presence of one equivalent CB7 (15  $\mu\text{M}$ ); the absorption spectra were normalized to 1 at  $\lambda_{\text{max}}$ . Bottom: Kinetic decays of the colored linear form in the absence (black dots) or presence of CB7 (one equivalent; red dots).

of  $\text{CB}_n$  is attributed to the increased steric screening around the amino moiety as the principal factor. We presume that the steric overload has its main impact on the C3–C4 bond rotation ( $\text{A}' \rightarrow \text{A}''$ ) and the  $4\pi$  electrocyclicization ( $\text{A}'' \rightarrow \text{B}'$ ); see Scheme 1.<sup>7,13,32</sup> In addition, the above-mentioned stabilization of the CT state by ion–dipole interactions with the  $\text{CB}_n$  macrocycles could be another contribution to the reduced “dark switching”.

The experimental observations are in very good agreement with theoretical calculations [M06-2X/def2-SVP/CPCM-(water) level of theory]<sup>41,42</sup> of the reaction path in the absence and presence of  $\text{CB}_7$  (Figure 3). For example, for the

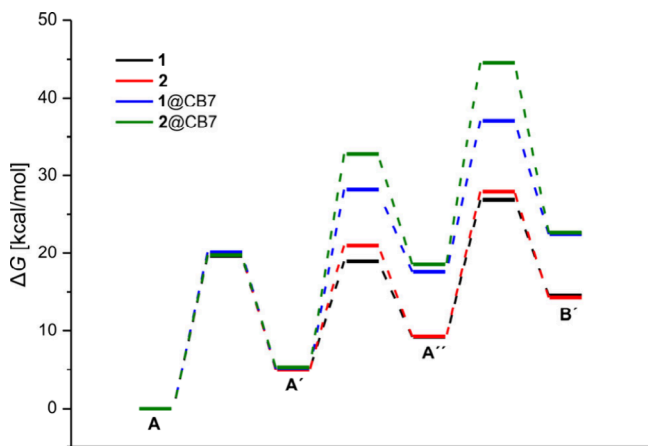


**Figure 3.** Calculated energy profile for the “dark switching” of DASA 1 and 2 and their  $\text{CB}_7$  complexes in water.

case of DASA 1 the calculations predict an increase of the activation barrier by about  $9.1 \text{ kcal mol}^{-1}$  for the  $\text{A}' \rightarrow \text{A}''$  step of the supramolecular complex. For DASA 2, which experiences even more dramatic stabilization of the linear form, the energy barrier for the  $\text{A}' \rightarrow \text{A}''$  step raises by  $11.4 \text{ kcal mol}^{-1}$  as compared to the free dye (Figure 3 and Supporting Information, Table S3 and Figures S39–S42). In addition, the energy barrier for the  $\text{A}'' \rightarrow \text{B}'$  transformation is raised significantly by  $7.4 \text{ kcal mol}^{-1}$  for DASA 2 in the presence of  $\text{CB}_7$ .

Next, we investigated the photoswitching of the DASA dyes. Upon irradiation at wavelengths  $>455 \text{ nm}$ , the free dyes showed decolorization, characterized by the disappearance of the  $\pi, \pi^*$  absorption band and the build-up of the closed cyclopentenone isomer with UV absorption below  $300 \text{ nm}$  (Supporting Information, Figures S26 and S27). It should be noted that the photoinduced ring closing proceeds about 10 times faster than the “dark switching”. The photoreaction of 1 and 2 proceeded with a global quantum yield  $\Phi_r$  of 0.03 and 0.06, respectively. However, for the supramolecular  $\text{CB}_7$  and  $\text{CB}_8$  complexes a pronounced drop in the efficiency was observed, being  $\Phi_r < 0.005$  (Supporting Information, Figures S31–S34). This reflects the increased steric congestion of the host-encapsulated amine donor moiety, interfering in the thermal steps of the mechanism,<sup>7</sup> akin to the observations for the “dark switching” (see above). However, the photoswitching can be still carried out conveniently on a time scale of a few minutes (see below).

Finally, we sought to achieve reversible T-type photoswitching of the systems. We irradiated the  $\text{CB}_7$  complex of 1 for time periods of 30–150 s with visible light ( $>455 \text{ nm}$ , at room temperature). For the longest irradiation time a conversion of *ca.* 20% was reached. After switching off the lamp the colored linear form was recovered with a  $t_{1/2}$  of *ca.* 50 s (Figure 4). For the  $\text{CB}_7$  complex of DASA 2 the same experiment was performed and a comparable conversion level was observed (Supporting Information, Figure S35). However, the thermal back reaction was not spontaneous at room temperature and heating to  $55 \text{ }^\circ\text{C}$  was necessary to recover the colored linear form. Even then the recovery time was in the order of several minutes. This observation goes along with the considerably higher energetic barrier (difference of  $7.2 \text{ kcal mol}^{-1}$ ) for the electrocyclic reversion of the cyclopentenone of 2 as compared to 1 ( $\text{B}' \rightarrow \text{A}''$  in Scheme 1); see the Supporting Information, Table S3. For the  $\text{CB}_8$  complexes of 1 and 2 a similar switching behavior as for the  $\text{CB}_7$  complexes was observed (Figure 4 and Supporting Information, Figure S36), including the need to heat to  $55 \text{ }^\circ\text{C}$  in the case of 2.

It is noteworthy that for the prolonged irradiation of the  $\text{CB}_8$  complex of 2 for 600 s about 33% of the linear form was transformed. This surpasses the best performing DASA in aqueous solution, for which *ca.* 20% conversion was observed under comparable conditions.<sup>28</sup> To compare the switching behavior in water with that of the DASA dyes alone in nonpolar organic medium, experiments in toluene were performed. For both dyes 1 and 2 the expected T-type switching was observed (Supporting Information, Figures S37 and S38). The half-life of the recovery of the linear form is in the order of tens to one hundred seconds ( $t_{1/2}$  *ca.* 25 s for 1 and 107 s for 2), that is in the same range as for  $\text{CB}_7$ - or  $\text{CB}_8$ -stabilized DASA 1 in water.

In conclusion, the supramolecular binding of the amine donor of DASA by cucurbit[*n*]urils exerts steric effects that

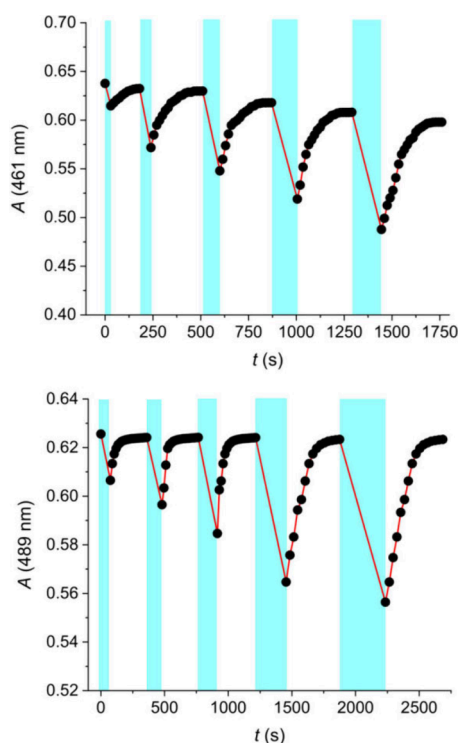


**Figure 4.** Switching of DASA 1 in the presence of 1 equiv CB7 (top) or CB8 (bottom) in water. Irradiation at  $>455$  nm for variable times (cyan bars; 0.5, 1, 1.5, 2, 2.5 min for CB7 and 1, 2, 2.5, 4, 5 min for CB8) and ring opening at room temperature. The systems show robust recovery over five cycles.

favor the stabilization of the colored linear form of first-generation DASA and their reversible photoswitching in water. Importantly, the proposed supramolecular approach is potentially compatible with other macrocycles than the herein employed cucurbit[*n*]urils, e.g., persulfonated pillar[6]arenes that form ultrastable host–guest complexes with adamantane binding motifs.<sup>43</sup>

## ■ ASSOCIATED CONTENT

### SI Supporting Information

The Supporting Information is available free of charge at <https://pubs.acs.org/doi/10.1021/jacs.5c19813>.

Experimental section, synthesis and characterization of DASA 1 and DASA 2, mass spectra of host–guest complexes, additional data on “dark switching” and reversible photoswitching of DASA dyes and their host–guest complexes with CB7 and CB8, fluorescence emission of DASA host–guest complexes with CB7 and CB8, and details about theoretical calculations (PDF)

Atomic coordinates of all calculated structures (TXT)

## ■ AUTHOR INFORMATION

### Corresponding Authors

**Michal Rouchal** – Department of Chemistry, Faculty of Technology, Tomas Bata University in Zlín, 760 01 Zlín, Czech Republic; [orcid.org/0000-0002-0117-4040](https://orcid.org/0000-0002-0117-4040); Email: [rouchal@utb.cz](mailto:rouchal@utb.cz)

**Uwe Pischel** – CIQSO – Center for Research in Sustainable Chemistry and Department of Chemistry, University of

Huelva, E-21071 Huelva, Spain; [orcid.org/0000-0001-8893-9829](https://orcid.org/0000-0001-8893-9829); Email: [uwe.pischel@diq.uhu.es](mailto:uwe.pischel@diq.uhu.es)

## Authors

**Francisco G. Blandón-Cumbreras** – CIQSO – Center for Research in Sustainable Chemistry and Department of Chemistry, University of Huelva, E-21071 Huelva, Spain

**Marek Jurtík** – Department of Chemistry, Faculty of Technology, Tomas Bata University in Zlín, 760 01 Zlín, Czech Republic

**Aneta Závadná** – Department of Chemistry, Faculty of Technology, Tomas Bata University in Zlín, 760 01 Zlín, Czech Republic

**Petr Janovský** – Department of Chemistry, Faculty of Technology, Tomas Bata University in Zlín, 760 01 Zlín, Czech Republic; [orcid.org/0009-0000-1040-965X](https://orcid.org/0009-0000-1040-965X)

**Robert Vicha** – Department of Chemistry, Faculty of Technology, Tomas Bata University in Zlín, 760 01 Zlín, Czech Republic; [orcid.org/0009-0003-8726-3232](https://orcid.org/0009-0003-8726-3232)

Complete contact information is available at:

<https://pubs.acs.org/10.1021/jacs.5c19813>

## Notes

The authors declare no competing financial interest.

## ■ ACKNOWLEDGMENTS

The authors acknowledge the funding of this work by the Spanish Ministry for Science, Innovation, and Universities (MCIU/AEI/10.13039/501100011033) and the European Regional Development Fund ERDF (grants PID2020-119992GB-I00 and PID2023-152556NB-I00 and predoctoral contract PRE2023-001520 for F.G.B.-C.) as well as the Internal Funding Agency of the Tomas Bata University in Zlín (project IGA/FT/2025/001). Funding for open access charge: Universidad de Huelva / CBUA.

## ■ REFERENCES

- (1) Feringa, B. L.; Browne, W. R. *Molecular Switches*, 2 Vol. Set; John Wiley & Sons: 2011.
- (2) Pianowski, Z. L. *Molecular Photoswitches: Chemistry, Properties, and Applications*, 2 Vol. Set; John Wiley & Sons: 2022.
- (3) Helmy, S.; Leibfarth, F. A.; Oh, S.; Poelma, J. E.; Hawker, C. J.; Read de Alaniz, J. Photoswitching Using Visible Light: A New Class of Organic Photochromic Molecules. *J. Am. Chem. Soc.* **2014**, *136*, 8169–8172.
- (4) Helmy, S.; Oh, S.; Leibfarth, F. A.; Hawker, C. J.; Read de Alaniz, J. Design and Synthesis of Donor–Acceptor Stenhouse Adducts: A Visible Light Photoswitch Derived from Furfural. *J. Org. Chem.* **2014**, *79*, 11316–11329.
- (5) Lerch, M. M.; Wezenberg, S. J.; Szymanski, W.; Feringa, B. L. Unraveling the Photoswitching Mechanism in Donor–Acceptor Stenhouse Adducts. *J. Am. Chem. Soc.* **2016**, *138*, 6344–6347.
- (6) Di Donato, M.; Lerch, M. M.; Lapini, A.; Laurent, A. D.; Iagatti, A.; Bussotti, L.; Ihrig, S. P.; Medved', M.; Jacquemin, D.; Szymanski, W.; Buma, W. J.; Foggi, P.; Feringa, B. L. Shedding Light on the Photoisomerization Pathway of Donor–Acceptor Stenhouse Adducts. *J. Am. Chem. Soc.* **2017**, *139*, 15596–15599.
- (7) Zulfikri, H.; Koenis, M. A. J.; Lerch, M. M.; Di Donato, M.; Szymanski, W.; Filippi, C.; Feringa, B. L.; Buma, W. J. Taming the Complexity of Donor–Acceptor Stenhouse Adducts: Infrared Motion Pictures of the Complete Switching Pathway. *J. Am. Chem. Soc.* **2019**, *141*, 7376–7384.
- (8) Clerc, M.; Sandlass, S.; Rifaie-Graham, O.; Peterson, J. A.; Bruns, N.; Read de Alaniz, J.; Boesel, L. F. Visible Light-Responsive Materials: The (Photo)chemistry and Applications of Donor–

Acceptor Stenhouse Adducts in Polymer Science. *Chem. Soc. Rev.* **2023**, *52*, 8245–8294.

(9) Hemmer, J. R.; Poelma, S. O.; Treat, N.; Page, Z. A.; Dolinski, N. D.; Diaz, Y. J.; Tomlinson, W.; Clark, K. D.; Hooper, J. P.; Hawker, C.; Read de Alaniz, J. Tunable Visible and Near Infrared Photoswitches. *J. Am. Chem. Soc.* **2016**, *138*, 13960–13966.

(10) Mallo, N.; Brown, P. T.; Iranmanesh, H.; MacDonald, T. S. C.; Teusner, M. J.; Harper, J. B.; Ball, G. E.; Beves, J. E. Photochromic Switching Behaviour of Donor–Acceptor Stenhouse Adducts in Organic Solvents. *Chem. Commun.* **2016**, *52*, 13576–13579.

(11) Hemmer, J. R.; Page, Z. A.; Clark, K. D.; Stricker, F.; Dolinski, N. D.; Hawker, C. J.; Read de Alaniz, J. Controlling Dark Equilibria and Enhancing Donor–Acceptor Stenhouse Adduct Photoswitching Properties through Carbon Acid Design. *J. Am. Chem. Soc.* **2018**, *140*, 10425–10429.

(12) Lerch, M. M.; Medved', M.; Lapini, A.; Laurent, A. D.; Iagatti, A.; Bussotti, L.; Szymański, W.; Buma, W. J.; Foggi, P.; Di Donato, M.; Feringa, B. L. Tailoring Photoisomerization Pathways in Donor–Acceptor Stenhouse Adducts: The Role of the Hydroxy Group. *J. Phys. Chem. A* **2018**, *122*, 955–964.

(13) Mallo, N.; Foley, E. D.; Iranmanesh, H.; Kennedy, A. D. W.; Luis, E. T.; Ho, J.; Harper, J. B.; Beves, J. E. Structure–Function Relationships of Donor–Acceptor Stenhouse Adduct Photochromic Switches. *Chem. Sci.* **2018**, *9*, 8242–8252.

(14) Peterson, J. A.; Stricker, F.; Read de Alaniz, J. Improving the Kinetics and Dark Equilibrium of Donor–Acceptor Stenhouse Adduct by Triene Backbone Design. *Chem. Commun.* **2022**, *58*, 2303–2306.

(15) Reyes, C. A.; Lee, H. J.; Karanovic, C.; Picazo, E. Development and Characterization of Amino Donor–Acceptor Stenhouse Adducts. *Nat. Commun.* **2024**, *15*, 5533.

(16) Li, Z.; Wang, Z.; Chen, X.; Bao, J.; Zhang, Y.; Wang, Z.; Zhang, L.; Xiao, J.; Lan, R.; Yang, H. Reconfigurable Visible Light-Driven Liquid Crystalline Network Showing Off-Equilibrium Motions Enabled by Mesogen-Grafted Donor–Acceptor Stenhouse Adducts. *Adv. Mater.* **2024**, *36*, 2411530.

(17) Liu, B.; Fan, X.; Ma, H.; Xie, Y.; Fan, H.; Yan, Q.; Xiang, J. A DASA Displaying Highly Efficient and Rapid Reversible Isomerization Within Sustainable Nano/Micro Capsules: One Step Closer to Sustainability. *Chem. Sci.* **2024**, *15*, 17200–17209.

(18) Sun, F.; Gao, A.; Yan, B.; Zhang, J.; Wang, X.; Zhang, H.; Dai, D.; Zheng, Y.; Deng, X.; Wei, C.; Wang, D. Self-Adaptive Photochromism. *Sci. Adv.* **2024**, *10*, No. eads2217.

(19) Lerch, M. M.; Hansen, M. J.; Velema, W. A.; Szymanski, W.; Feringa, B. L. Orthogonal Photoswitching in a Multifunctional Molecular System. *Nat. Commun.* **2016**, *7*, 12054.

(20) Poelma, S. O.; Oh, S. S.; Helmy, S.; Knight, A. S.; Burnett, G. L.; Soh, H. T.; Hawker, C. J.; Read de Alaniz, J. Controlled Drug Release to Cancer Cells from Modular One-Photon Visible Light-Responsive Micellar System. *Chem. Commun.* **2016**, *52*, 10525–10528.

(21) Yap, J. E.; Zhang, L.; Lovegrove, J. T.; Beves, J. E.; Stenzel, M. H. Visible Light–Responsive Drug Delivery Nanoparticle via Donor–Acceptor Stenhouse Adducts (DASA). *Macromol. Rapid Commun.* **2020**, *41*, 2000236.

(22) Diaz, Y. J.; Page, Z. A.; Knight, A. S.; Treat, N. J.; Hemmer, J. R.; Hawker, C. J.; Read de Alaniz, J. A Versatile and Highly Selective Colorimetric Sensor for the Detection of Amines. *Chem.—Eur. J.* **2017**, *23*, 3562–3566.

(23) Cai, Y.-D.; Chen, T.-Y.; Chen, X. Q.; Bao, X. Multiresponsive Donor–Acceptor Stenhouse Adduct: Opportunities Arise from a Diamine Donor. *Org. Lett.* **2019**, *21*, 7445–7449.

(24) Castagna, R.; Maleeva, G.; Pirovano, D.; Matera, C.; Gorostiza, P. Donor–Acceptor Stenhouse Adduct Displaying Reversible Photoswitching in Water and Neuronal Activity. *J. Am. Chem. Soc.* **2022**, *144*, 15595–15602.

(25) Volarić, J.; Szymanski, W.; Simeth, N. A.; Feringa, B. L. Molecular Photoswitches in Aqueous Environments. *Chem. Soc. Rev.* **2021**, *50*, 12377–12449.

(26) Reyes, C. A.; Karr, A.; Ramsperger, C. A.; K, A. T. G.; Lee, H. J.; Picazo, E. Compartmentalizing Donor–Acceptor Stenhouse Adducts for Structure–Property Relationship Analysis. *J. Am. Chem. Soc.* **2025**, *147*, 10–26.

(27) Wang, D.; Zhao, L.; Zhao, H.; Wu, J.; Wagner, M.; Sun, W.; Liu, X.; Miao, M.; Zheng, Y. Inducing Molecular Isomerization Assisted by Water. *Commun. Chem.* **2019**, *2*, 118.

(28) Peterson, J. A.; Neris, N. M.; Read de Alaniz, J. Tethered Together: DASA Design Towards Aqueous Compatibility. *Chem. Sci.* **2023**, *14*, 13025–13030.

(29) Payne, L.; Josephson, J. D.; Murphy, R. S.; Wagner, B. D. Photophysical Properties of Donor–Acceptor Stenhouse Adducts and Their Inclusion Complexes with Cyclodextrins and Cucurbit[7]uril. *Molecules* **2020**, *25*, 4928.

(30) Mukhopadhyay, S.; Sarkar, A.; Ghoshal, S.; Sarkar, P.; Dhara, K.; Chattopadhyay, P. Encapsulation and Stabilization of a Donor–Acceptor Stenhouse Adduct Isomer in Water Inside the Blue Box: A Combined Experimental and Theoretical Approach. *J. Phys. Chem. B* **2021**, *125*, 7222–7230.

(31) Puthoff, D.; Kuttilyil, H.; Peterson, J. A. Stenhouse Salts: Visible Light Photoswitches for Protic Environments. *J. Am. Chem. Soc.* **2024**, *146*, 34008–34013.

(32) Stricker, F.; Sanchez, D. M.; Raucci, U.; Dolinski, N. D.; Zayas, M. S.; Meisner, J.; Hawker, C. J.; Martínez, T. J.; Read de Alaniz, J. A Multi-Stage Single Photochrome System for Controlled Photoswitching Responses. *Nat. Chem.* **2022**, *14*, 942–948.

(33) Assaf, K. I.; Nau, W. M. Cucurbiturils: From Synthesis to High-Affinity Binding and Catalysis. *Chem. Soc. Rev.* **2015**, *44*, 394–418.

(34) Barrow, S. J.; Kasera, S.; Rowland, M. J.; del Barrio, J.; Scherman, O. A. Cucurbituril-Based Molecular Recognition. *Chem. Rev.* **2015**, *115*, 12320–12406.

(35) Ghosh, I.; Nau, W. M. The Strategic Use of Supramolecular  $pK_a$  Shifts to Enhance the Bioavailability of Drugs. *Adv. Drug Delivery Rev.* **2012**, *64*, 764–783.

(36) Alnajjar, M. A.; Nau, W. M.; Hennig, A. A Reference Scale of Cucurbit[7]uril Binding Affinities. *Org. Biomol. Chem.* **2021**, *19*, 8521–8529.

(37) Grimme, S.; Hansen, A.; Ehlert, S.; Mewes, J.-M.  $r^2$ SCAN-3c: A “Swiss Army Knife” Composite Electronic-Structure Method. *J. Chem. Phys.* **2021**, *154*, 064103.

(38) Neese, F. Software Update: The ORCA Program System, Version 5.0. *WIREs Comput. Mol. Sci.* **2022**, *12*, No. e1606.

(39) Lerch, M. M.; Szymański, W.; Feringa, B. L. The (Photo)-chemistry of Stenhouse Photoswitches: Guiding Principles and System Design. *Chem. Soc. Rev.* **2018**, *47*, 1910–1937.

(40) Sroda, M. M.; Stricker, F.; Peterson, J. A.; Bernal, A.; Read de Alaniz, J. Donor–Acceptor Stenhouse Adducts: Exploring the Effects of Ionic Character. *Chem.—Eur. J.* **2021**, *27*, 4183–4190.

(41) Zhao, Y.; Truhlar, D. G. The M06 Suite of Density Functionals for Main Group Thermochemistry, Thermochemical Kinetics, Noncovalent Interactions, Excited States, and Transition Elements: Two New Functionals and Systematic Testing of Four M06-Class Functionals and 12 Other Functionals. *Theor. Chem. Acc.* **2008**, *120*, 215–241.

(42) Bannwarth, C.; Caldeweyher, E.; Ehlert, S.; Hansen, A.; Pracht, P.; Seibert, J.; Spicher, S.; Grimme, S. Extended Tight-Binding Quantum Chemistry Methods. *WIREs Comput. Mol. Sci.* **2021**, *11*, No. e1493.

(43) Xue, W.; Zavalij, P. Y.; Isaacs, L. Pillar[n]MaxQ: A New High Affinity Host Family for Sequestration in Water. *Angew. Chem., Int. Ed.* **2020**, *59*, 13313–13319.